

We are IntechOpen, the world's leading publisher of Open Access books Built by scientists, for scientists

6,900

Open access books available

185,000

International authors and editors

200M

Downloads

Our authors are among the

154

Countries delivered to

TOP 1%

most cited scientists

12.2%

Contributors from top 500 universities



WEB OF SCIENCE™

Selection of our books indexed in the Book Citation Index
in Web of Science™ Core Collection (BKCI)

Interested in publishing with us?
Contact book.department@intechopen.com

Numbers displayed above are based on latest data collected.
For more information visit www.intechopen.com



Development of Semiclosed Cycle Gas Turbine for Oxy-Fuel IGCC Power Generation with CO₂ Capture

Takeharu Hasegawa

Additional information is available at the end of the chapter

<http://dx.doi.org/10.5772/54406>

1. Introduction

In response to recent changes in energy-intensive and global environmental conditions, it is urgent and crucial concern to develop the high-efficiency technologies of fossil fuel power generations. Especially, coal is one of the most important resources from the standpoint of risk avoidance in the scheme of power supply composition. Figure 1 shows the proved recoverable reserves of coal by region compared with those of the natural gas and crude oil. The world's coal reserves are twice that of each conventional oil and natural gas, distributed more evenly on a geographical basis than those for oil and natural gas, and also geopolitical risk is lower for securing the stable supply of coal resource. This figure also shows each total discoverable reserve of non-conventional resources of natural gas and crude oil as references, and each reserve corresponds to twice of the coal proved recoverable reserve. In this regard, however, total discoverable reserve of coal is estimated ten times of proved recoverable reserves, or it corresponds to five times of that of each non-conventional resource of natural gas and crude oil. Coal is definitely the most important fossil fuel resources in the future.

Furthermore, in the 1997 when the Third Conference of Parties to the United Nations Framework Convention on Climate Change (COP3), the Kyoto protocol, which invoked mandatory CO₂ emissions reductions on countries, was adopted. CO₂ emissions per unit calorie of coal are about 1.8 times that in the case of natural gas, and then CO₂ recovery technologies are very important for thermal power plants.

On the other hand, demand of coal has increased rapidly in the recent years. Figure 2 shows annual changes of the world's coal consumption by region and the reserves-to-production ratios of coal, oil and natural gas. In the intervening quarter-century from 1985 to 2010, the coal consumption in Asia Pacific increased significantly or about 3.6 times, while world coal

consumption increased 1.7 times. The increase in coal consumption in Asia Pacific is equal to one half of the world's consumption in 2010, while consumptions in other regions decrease. In just ten years, coal consumption in Asia Pacific increased double, and then the world's reserves-to-production ratio of coal decreased by half, while the reserves-to-production ratios of oil and natural gas have been maintained constant. Along with the growing world demands for fossil energy resources in recent years, international competition for development of fossil fuel fields of coal, oil and gas in the world is ever intensified.

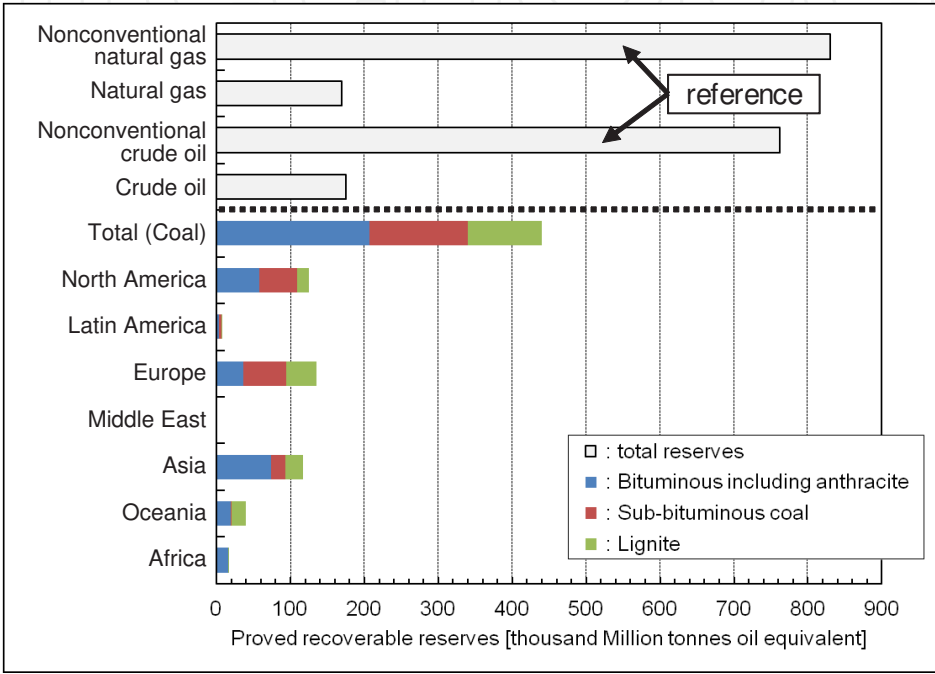


Figure 1. Proved recoverable reserves of coal by region at end 2010, compared with oil and natural gas reserves. Source of reserves data: BP statistical review of world energy 2011 [1]. Notes: Coal proved reserves expressed in tonnes oil equivalent are calculated using coal productions based on data expressed in tonnes oil equivalent and coal productions in tonnes. Nonconventional natural gas shows data not including methane hydrate reserves. Nonconventional crude oil includes oil shale and oil sand reserves.

With the above mentioned situations as a background, developments of high-efficiency power generation technologies and low emission technologies of CO₂ become increasingly important in the world. As one of the highly-efficient and low CO₂ emission technologies, an integrated coal gasification combined cycle (IGCC) power generation combined with CO₂ capture and storage (CCS) technologies are now drawing attention from the electric power industry. The Central Research Institute of Electric Power Industry (CRIEPI) has proposed a newly-designed oxy-fuel IGCC power generation system integrated with a combination of CO₂ recovery processing and a semiclosed cycle gas turbine [3]. This system wields the advantages of not requiring a CO₂ capture system using CO₂ absorption processing or fuel reforming preprocessing. Compared to conventional CO₂ recovery thermal power plants, oxy-fuel IGCC could simplify CO₂ recovery systems, reduce station service power, and achieve higher thermal efficiency. Currently, CRIEPI is addressing each technological development

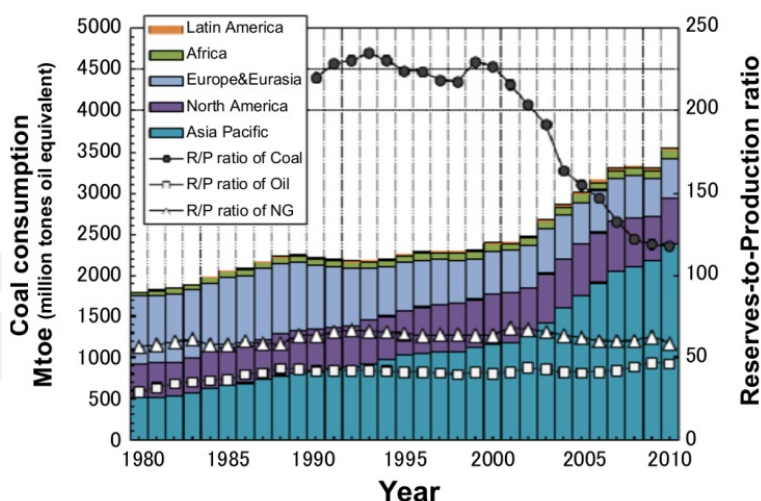


Figure 2. World coal consumption by region and proved recoverable reserves-to-production (R/P) ratio of coal, oil and natural gas (NG) at end 2010. Note: Coal data include anthracite, bituminous, sub-bituminous, and lignite. And reserves-to-production (R/P) ratios are approximate values based on the total proved recoverable reserves of bituminous coal, anthracite, lignite and sub-bituminous coal. Sources are BP statistical review of world energy [1] and data reported for precious World Energy Council Surveys of Energy Resources [2].

[4-9] towards the realization of highly efficient power generation with zero emissions, and with a semiclosed gas turbine system serving as one of the key technologies.

In this study, we have been researching and developing the combustion technologies in order to achieve the semiclosed cycle gas turbine for highly efficient oxy-fuel IGCC [5-6]. This paper describes technical difficulties and combustion characteristics of semiclosed gas turbine combustors, comparing developed H₂/O₂ and natural gas/O₂ fired semiclosed gas turbines in the WE-NET project [10] and a conventional natural gas fired gas turbine.

2. CO₂ recovery from thermal power plant

2.1. CO₂ recovery methods for IGCCs

Along with the oxy-fuel IGCC system newly proposed in this paper, there exist four CO₂ recovery systems for coal-base thermal power generation. With regard to CO₂ recovery systems for IGCC, as shown in figure 3, the oxy-fuel IGCC system and the pre-combustion system for IGCC are under development [11-14]. In the case of an oxy-fuel IGCC power generation system with CO₂ capture in a semiclosed cycle oxy-fuel gas turbine, recovery of CO₂ is simplified, with decreasing station service power expected to produce highly efficient generation. This is because water-gas-shift reactors and physical/chemical solvents for CO₂ capture are not required as opposed to conventional pre-combustion systems for IGCC.

Figure 4 shows the change in net plant efficiency (HHV basis) in conventional pulverized coal and IGCC power plants. In the case of 90 percent CO₂-recovery, post-combustion systems, the thermal efficiency of pulverized-coal, super critical boilers decreases to 28.4% [11]

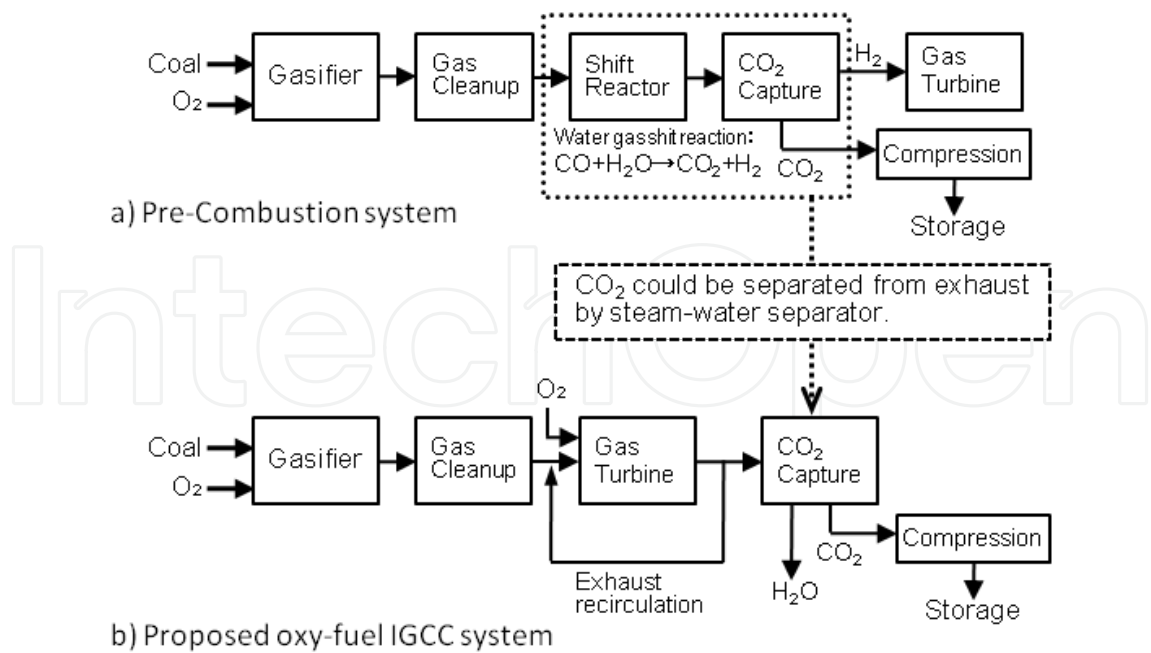


Figure 3. Comparison of CO₂ recovery processes for IGCCs

from 39.3% since a huge amount of steam is needed to regenerate absorbers, while oxy-fuel combustion systems of O₂-fired pulverized coal boilers result in only a marginal improvement in thermal efficiency of 29.3% [11]. Furthermore, in the case of a pre-combustion system using an F-class gas turbine for IGCC, thermal efficiency is expected to improve to 31.6% [11].

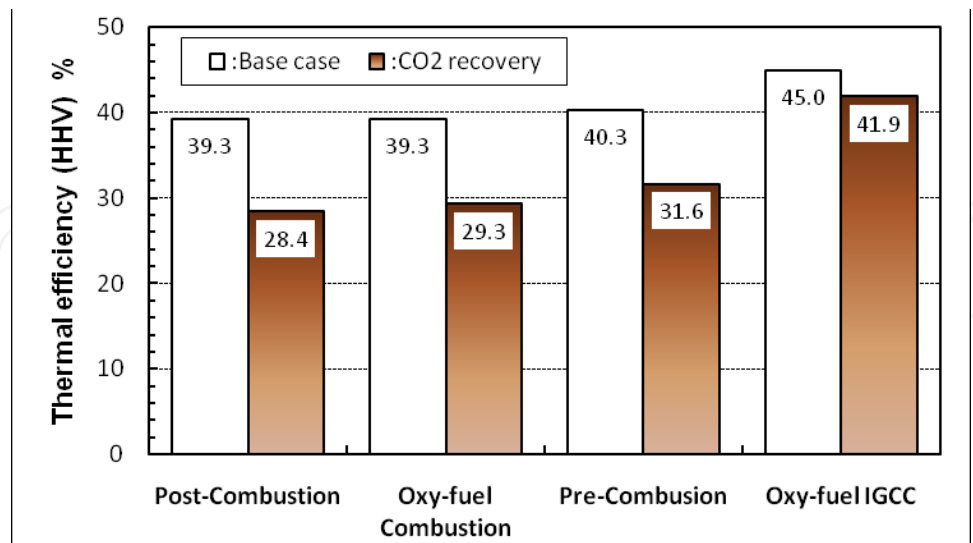


Figure 4. Thermal efficiency of coal-base power plants with and without CO₂ capture and compression. In the three conventional cases of post-, oxy-fuel and pre-combustion, currently available technologies are employed and CO₂ recovery rate is set at 90% [11]. In the case of oxy-fuel IGCC employing technologies currently under development, CO₂ recovery rate is set at 99% [4].

However, in the case of an oxy-fuel IGCC system adopting each technology currently under development, the use of an O₂-CO₂ gasifier, for example, with a hot/dry synthetic gas clean-up system and a semiclosed cycle gas turbine (turbine inlet temperature on ISO standard basis at about 1530K), is expected to produce a transmission-end thermal efficiency of 41.9% under conditions of 99% or higher CO₂ recovery.

2.2. Oxy-fuel IGCC and closed-cycle gas turbine

Figure 5 shows a schematic diagram of the oxy-fuel IGCC system and a topping semiclosed cycle gas turbine. The newly proposed oxy-fuel IGCC consists of an oxygen-CO₂ blown gasifier, a hot/dry synthetic gas cleanup system, a semiclosed cycle oxygen-fired gas turbine, and a CO₂ recovery process. This system has the following advantages;

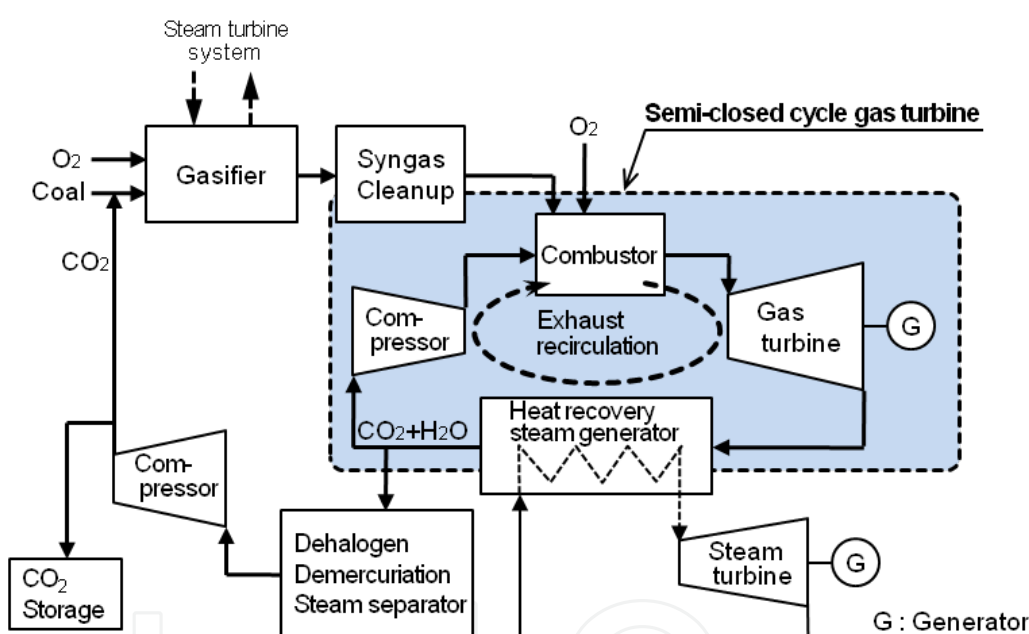


Figure 5. Schematic diagram of oxy-fuel IGCC and semiclosed cycle gas turbine [3]

- Oxygen- CO_2 blown, entrained-flow coal gasifier

Table 1 shows the rated conditions of a gasified fuel and semiclosed cycle gas turbine combustor [3],[4]. Table 2 shows characteristics of coal used in the calculation [3]. Here, we dry fed pulverized coal into an oxygen-blown entrained-flow gasifier with recycled CO_2 from flue gas, and gasified with additional oxygen. In addition, we found that O_2 - CO_2 blown coal gasification enhanced gasification efficiency compared to that of current oxygen blown gasification through dry feeding of coal with N_2 . Figure 6 shows the gasification characteristics of the two cases above, estimated by numerical analysis of a one-dimensional model [3].

| Components | Gasified fuel | Oxidizer | Dilution |
|---|--|----------|----------|
| CO [vol%] | 66.2 | 0 | 0 |
| H ₂ | 23.8 | 0 | 0 |
| CH ₄ | 0.3 | 0 | 0 |
| CO ₂ | 4.9 | 0 | 69.5 |
| H ₂ O | 3.2 | 0 | 26.9 |
| Ar, N ₂ | 1.5 | 2.5 | 2.7 |
| O ₂ | 0 | 97.5 | 0.9 |
| HHV (LHV) | 11.5 MJ/m ³ (11.0 MJ/m ³) at 273K, 0.1MPa | | |
| Pressure in combustor | 2.2MPa | | |
| ϕ * | 0.98 (Overall equivalence ratio ϕ is 0.89) | | |
| Dilution ratio | 5.5: dilution/fuel molar ratio | | |
| Exhaust temp. | 1573K at combustor exit | | |
| ϕ * : calculated from fuel and oxidizer without O ₂ concentration in dilution | | | |

Table 1. Rated conditions of semiclosed cycle gas turbine combustor [3],[4]

| | |
|-----------------------------------|------|
| Inherent moisture* [wt%] | 3.6 |
| Ash content* [wt%] | 9.6 |
| Volatile matter* [wt%] | 30.3 |
| Fixed carbon* [wt%] | 56.5 |
| Ultimate analysis** | |
| C [wt%] | 76.1 |
| H [wt%] | 5.1 |
| O [wt%] | 6.9 |
| N [wt%] | 1.7 |
| S [wt%] | 0.5 |
| *: air-dried state, **: dry basis | |

Table 2. Characteristics of coal used in calculation [3]

Table 3 shows numerical analysis conditions in gasification. Gasified fuels were calculated under conditions where an equivalence ratio in the gasification was set at 2.58 through multi-stage analyses utilizing pyrolysis, char gasification reaction and gas phase equilibrium reaction processes, and assuming a one-dimensional axial flow in the entrained-flow gasifier [3].We assumed that volatile matter contents in coal would be instantaneously pyrolyzed in

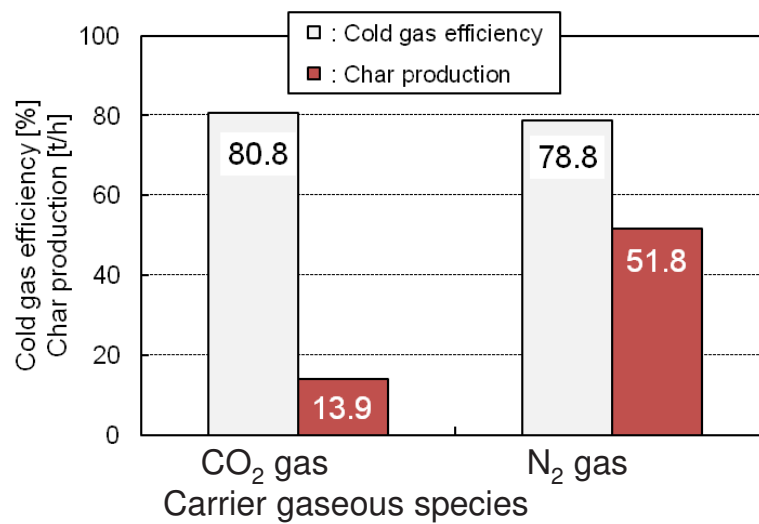


Figure 6. Influence of carrier gas conveying pulverized coal into gasifier on oxygen-blown gasification performance under conditions of coal input of 118.5t/h [3]

the first stage, so we took 3-step reduced reactions in char gasification into account. For char gasification, we used char reaction rates based on experimental data from a pressurized drop tube furnace [15]. In the analyses, we determined the point in time when char input accorded with char production to be equilibrium. Since we assumed 100% removal rates of dust and sulfur in the synthetic gas cleanup, gasified fuels shown in Table 1 did not include sulfur, halide, ash and metal impurities.

| Calculation | One-dimensional model |
|---|---|
| Reaction | |
| 1) Pyrolysis | |
| Coal → C _n H _m O _i + Char | Pyrolyzed instantaneously |
| 2) Reaction of Char | |
| C + 1/2O ₂ → CO | Reaction rates obtained from data in pressure drop tube furnace |
| C + CO ₂ → 2CO | |
| C + H ₂ O → CO+H ₂ | |
| 3) Gas phase reaction | |
| (C _n H _m O _i) → (CH ₄ , H ₂ , CO, CO ₂ , H ₂ O, N ₂ , O ₂) | Equilibrium reaction |

Table 3. Analysis method and conditions [3]

The cold gas efficiency in Fig.6 demonstrates the ratio between chemical energy content in the product gas compared to chemical energy in fuel on a lower heating value basis. Cold gas efficiency was calculated in the following way:

$$\text{cold gas efficiency} = \frac{\text{product gas}[\text{mass flow} \times \text{heating value}] - \text{additional fuel}[\text{mass flow} \times \text{heating value}]}{\text{coal supplied to gasifier}[\text{mass flow} \times \text{heating value}]} \times 100 \quad (1)$$

As a result, we estimated an improvement in cold gas efficiency by 2 percent and a reduction of char particles. At the same time, we clarified the influence of CO₂ and H₂O content on char production characteristics by using a pressurized drop tube furnace [8], and we evaluated the effects of CO₂ enrichment on coal gasification performance using an actual pressurized entrained flow coal gasifier of a 3ton/day bench scale gasifier [9]. Results confirmed that CO₂ enrichment improves gasification characteristics.

- Hot/dry synthetic gas cleanup

We treated gasified fuels with a hot/dry synthetic gas cleanup system consisting of a metallic filter, a hot gas desulfurization unit and other materials, which simplified the cleanup system and reduced the power consumption for cleanup [7]. Dust removal technologies using metallic filters or ceramic ones have already been demonstrated and put to practical use in IGCC plants. So far, the Central Research Institute of Electric Power Industry has developed a halide sorbent containing NaAlO₂ [16], a honeycomb zinc ferrite desulfurization sorbent containing ZnFe₂O₄ [7], a honeycomb copper based mercury sorbent containing CuS [17], and an ammonia decomposing Ni-based catalyst supported by ZSM-5 pellets [18] and each of those elemental technologies was expected to be applied to the hot/dry synthetic gas cleanup system for current IGCCs. Figure 7 [19] shows the schematics of the demonstration plant of the dry gas purification system for the IGCC now being developed. An ammonia catalytic removal process was expected to be installed following the desulfurization unit. The process sequence of the purification system was determined by considering the operation temperature and performance of the sorbents and catalyst. Recently, the Central Research Institute of Electric Power Industry has been moving ahead on design of a new dry gas purification system for the advanced oxy-fuel IGCC by applying the purification system employing the elemental technologies developed for current IGCCs. Impurities in gasified fuels such as dust, ash contents, metal compounds, sulfur, halide, mercury and others could be reduced to an allowable level [20] for conventional gas turbines.

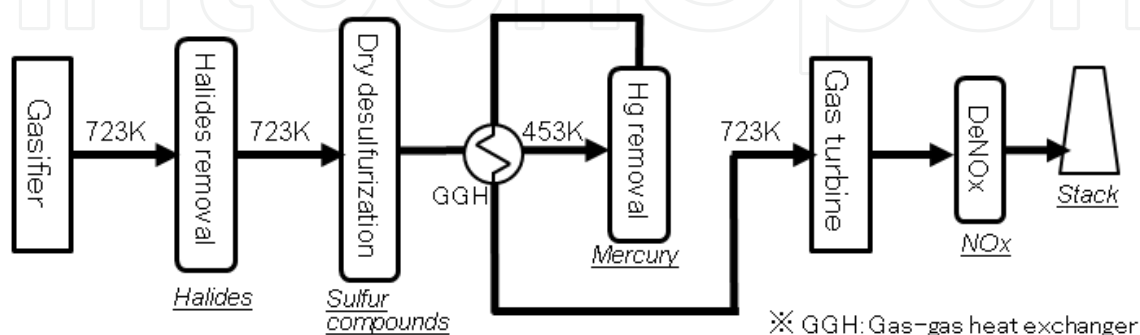


Figure 7. Schematic flow diagram of demonstration plant of dry gas purification system for current IGCCs [19]

- Semiclosed cycle gas turbine and CO₂ recovery

In a semiclosed cycle oxy-fuel gas turbine system as a topping cycle, we burned gasified fuels with pure oxygen and adjusted combustor exhaust temperature by recycling CO₂-enriched flue gas. As shown in Table 1, the rated temperature of combustor exhaust was set at 1573K (1300degC) and pressure inside the combustor at 2.2MPa [4]. After recovering exhaust heat in the HRSG, the necessary amount of flue gas was compressed and recycled to a gas turbine.

We then fed the remaining flue gas to a water scrubber of a halogen and Hg removal system and mist separator. We found that following these treatments, flue gas consisting mostly of CO₂ and H₂O became high-concentration CO₂ gas. We used some of the flue gas to feed coal to a gasifier, with the remainder compressed and sent to a storage site. It was necessary to reduce oxygen concentration in coal carrier gas to a low level in order to prevent pulverized coal from firing inappropriately.

Table 4 shows subjects and characteristics of gasified fuel/O₂ stoichiometric combustion with exhaust recirculation compared to a conventional natural gas-fired gas turbine. Unlike in the case of excess air combustion of an natural gas-fired gas turbine, the suppression of fuel oxidation under O₂-fired stoichiometric conditions with exhaust recirculation poses concerns, thereby necessitating the development of combustion promotion technology.

| | Oxy-fuel combustion in IGCC | Conventional natural gas-fire GT |
|---|--|-------------------------------------|
| Equivalence ratio | Stoichiometric (0.98) | 0.4~0.5 |
| | Oxidation reaction is restrained and unburned fuel is emitted. | at T _{ex} =1573K ~1773K |
| Dilution gas to adjust combustion temp. | Exhaust recirculation | Air |
| | Some exhaust is used as coal carrier gas, and then O ₂ concentration has to be decreased to a safe level. | |
| NOx emissions | Hot/dry cleanup and exhaust recirculation cause increased NOx emissions | Only thermal-NOx emissions |

Table 4. Subjects of semiclosed cycle gas turbine of gasified fuel/O₂ stoichiometric combustion with exhaust recirculation

In the case of oxy-fuel combustion in IGCC, a little excess O₂ combustion in which apparent equivalence ratio is set at 0.98 or lower resulted in higher concentrations of residual O₂ in exhaust, restraining the usage of exhaust to feed coal into the gasifier while combustion efficiency rose. And the presence of non-condensable gases such as remaining O₂, and Ar and N₂ separated from the air resulted in increased condensation duty for the recovery of the CO₂ [21]. On the other hand, a little higher equivalence ratio over stoichiometric conditions

decreased combustion efficiency. We have to accomplish higher combustion efficiency under almost stoichiometric conditions and decrease.

Furthermore, both the employment of hot/dry synthetic gas cleanup and exhaust recirculation increased fuel-NO_x emissions.

Against the above backdrop, we first of all researched combustion characteristics and exhaust gas reaction characteristics in the semiclosed cycle gas turbine for oxy-fuel IGCC [5].

3. Numerical analysis method based on elementary reaction models with PSR and PFR

We examined the reaction characteristics of reactant gases both in the combustor and in exhaust using numerical analysis based on the following elementary reaction kinetics. Here, we employed the reaction model proposed by Miller and Bowman [22], and confirmed by test result comparison the appropriateness of the model for non-catalytic reduction of ammonia in gasified fuel using NO [23] and an oxidation of ammonia by premixed methane flame [22].

The reaction scheme we employed was composed of 248 elementary reactions, with 50 species taken into consideration. Miller and Bowman described both a detailed scheme of the oxidation of C1 and C2 hydrocarbons under most (but not too fuel-rich) conditions, and an essential scheme for ammonia oxidation. Hasegawa et al. [23], united these two schemes and confirmed the applicable scope of a united scheme through experiments using a flow tube reactor. As an example, figure 8 shows comparative calculations results with non-catalytic denitration tests performed by Lion [24]. The analytical results precisely described a narrow reaction temperature for effective non-catalytic denitration and the behavior of NH₃ and NO constituents. Furthermore, the authors have evaluated the reaction characteristics of ammonia reduction in the gasified fuels, of non-catalytic denitration in exhaust, of air-fired gasified fueled combustions, and of H₂/O₂ stoichiometric combustion through experiments and full kinetic analyses [23], [25]-[27]. Results showed that the united scheme could describe the reaction characteristics in gasified fueled combustion and exhaust. On the other hand, various reaction schemes have been proposed worldwide for each reaction system including higher hydrocarbons. There was example of the GRI Mech 3.0 chemical kinetic mechanism used for calculation of the oxy-fuel gas turbine combustion [28]. But it need not be used since the gasified fuel contains a small percent of CH₄ and no C2 hydrocarbon.

We took thermodynamic data from the JANAF thermodynamics tables [29], and calculated the values of other species not listed in the tables based on the relationship between the Gibbs' standard energy of formation, ΔG° , and the chemical equilibrium constant, K , obtaining a value of ΔG° from the CHEMKIN database [30].

$$\Delta G^\circ = R \times T \times \ln(K) \quad (2)$$

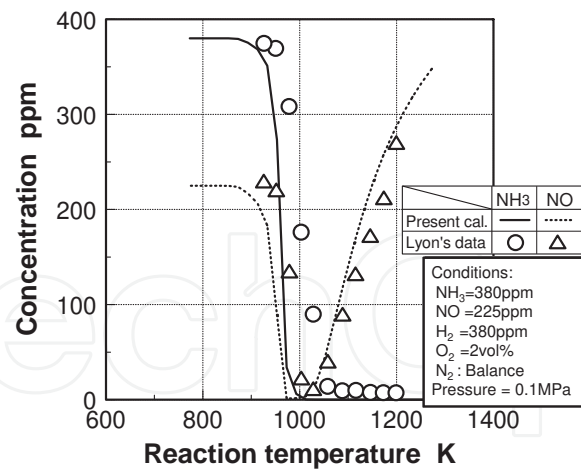


Figure 8. Comparison of kinetic analyses with experimental data of Lyon [24] on concentration of NH₃ and NO in the NH₃NOO₂H₂ system under conditions of selective nongatalytic reduction of NOx

We in this study used the GEAR method [31] for numerical analysis as an implicit, multi-stage solution.

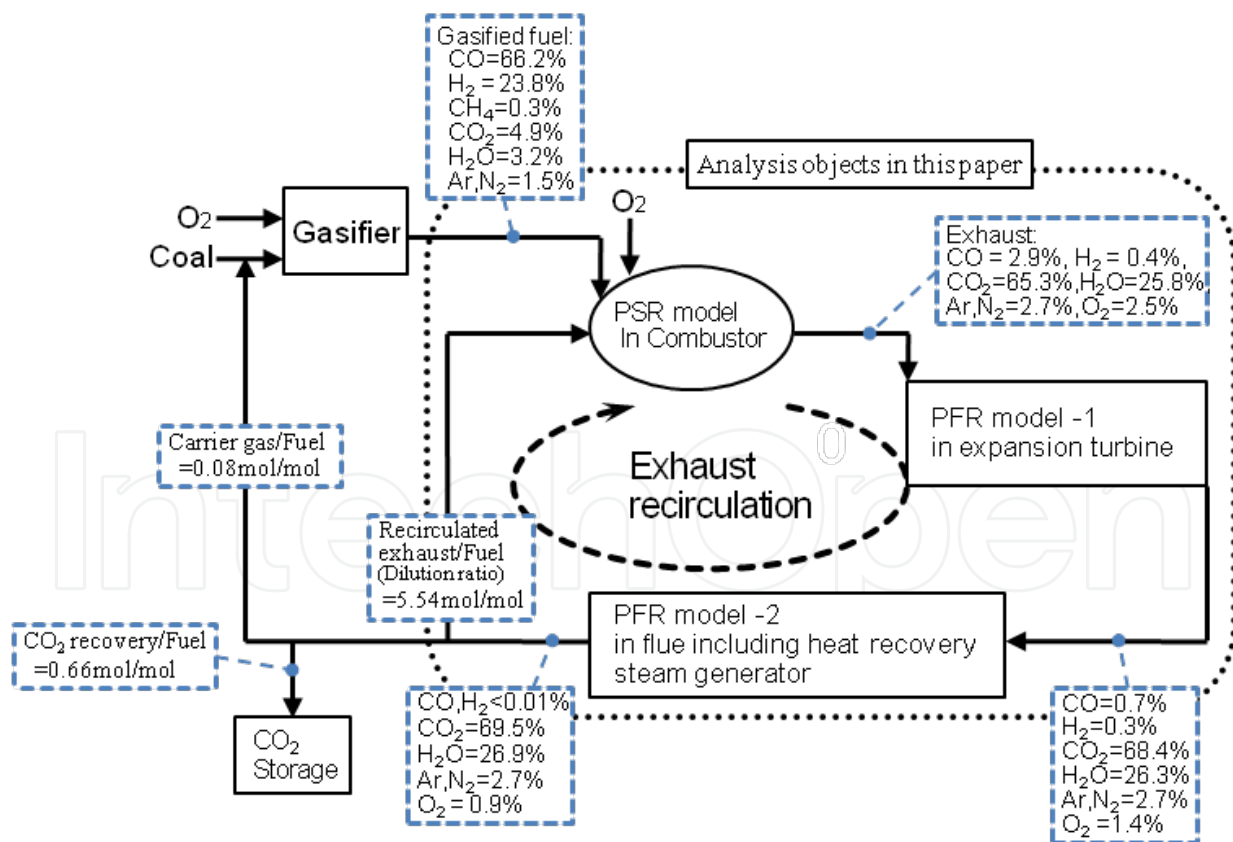


Figure 9. Schematic of algorithm in semiclosed gas turbine for oxy-fuel IGCC under typical rated conditions. Recirculated gas turbine exhaust is injected into the PSR of the combustor alongside incoming stream of gasified fuel and oxidizer of O₂.

Furthermore, our algorithm is schematized in Figure 9. The model we employed in this study assumed all mixing processes to be ideal such that they could be represented by a combination of a perfectly-stirred reactor (PSR) and a plug flow reactor (PFR). When investigating the basic combustion reaction characteristics that were independent of combustor geometries, the combustor was simply modeled as the PSR. This combustor model was the simplest case of modular models employed by Pratt, et al. [32]. In the case of investigating the exhaust gas reaction characteristics in expansion turbine and flue, we employed the PFR model. Then, we employed a combination PSR and PFR model in order to explore the influence of exhaust recirculation on combustor emission characteristics and exhaust reaction characteristics in the semiclosed gas turbine.

4. Characteristics of stoichiometric combustion with recirculating exhaust

4.1. Comparison with air-fired combustion

Figure 10 shows concentrations of principal chemical species against reaction time under the rated load conditions shown in Table 1, through a numerical analysis based on reaction kinetics with a PSR model of homogeneous reaction. Figure 11 also shows the principal chemical species against reaction time when burning CH_4 in the main components of natural gas with air under conditions where the reaction temperature is set at a constant value of the rated exhaust temperature of 1573K, and where the equivalence ratio is 0.32.

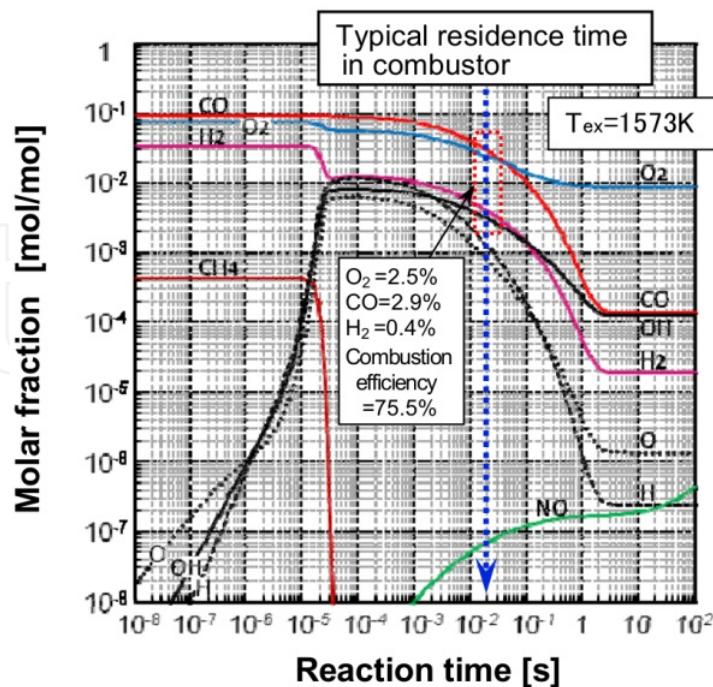


Figure 10. Chemical species behavior over time in gasified fuel/ O_2 stoichiometric combustion with exhaust recirculation

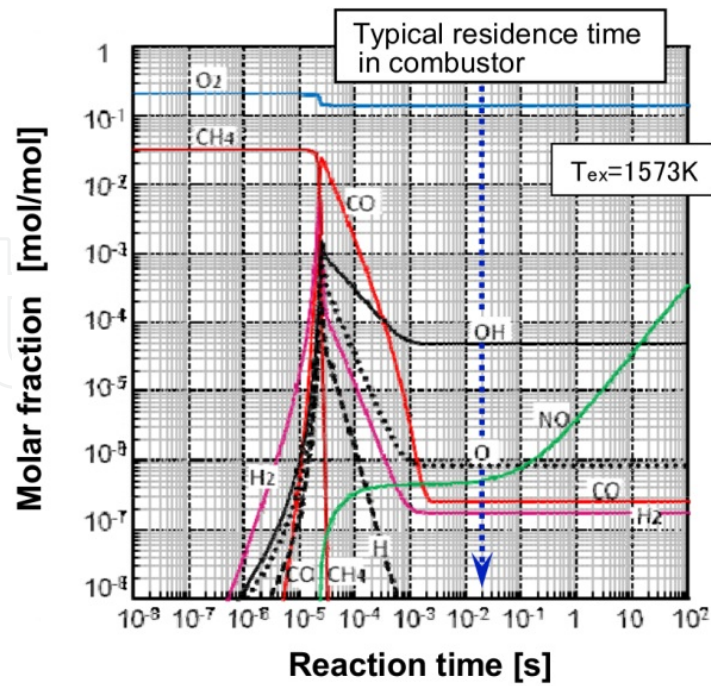


Figure 11. Chemical species behavior over time in conventional CH₄/air combustion

In the case of burning gasified fuel under stoichiometric conditions with exhaust recirculation, fuel oxidation reaction proceeded slowly compared to that of conventional CH₄/air combustion. As a result, we found that CO and H₂ in exhaust remained unoxidized at around 2.9vol% and 0.4vol%, respectively, and residual O₂ at 2.5vol% in 20ms corresponded to the combustion gas residence time in the combustor. Combustion efficiency was estimated to remain at a low level of around 76%, compared with that of conventional industrial gas turbines.

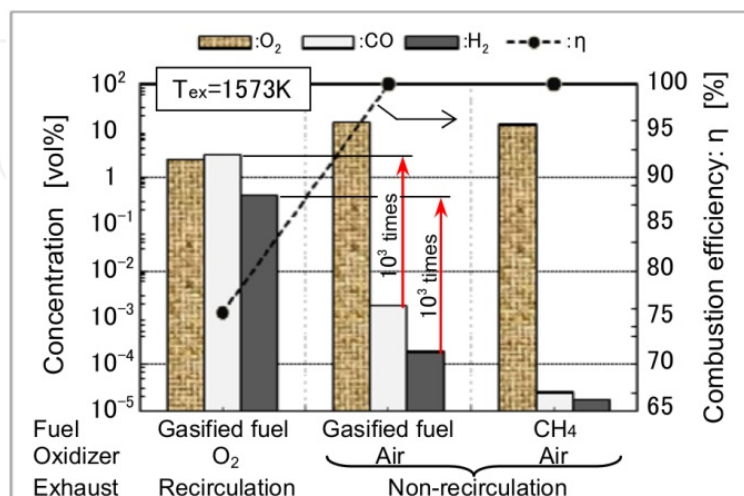


Figure 12. Comparison of emission characteristics with conventional air-fired combustions

Figure 12 shows exhaust characteristics and combustion efficiencies at the combustor exit under the conditions of a 1573K combustor exhaust temperature, in comparison with the homogeneous premixed combustion of a gasified fuel/air and CH₄/air mixture. The stoichiometric combustion of gasified fuel/O₂ with exhaust recirculation causes a drastic decrease in combustion efficiency compared with the other two cases of air-fired combustion. We feel that it is therefore necessary to promote fuel oxidation, or to decrease combustible constituent CO emitted from the gas turbine.

4.2. Comparison to each oxy-fuel gas turbine combustion

Figure 13 shows the results of numerical analysis in hydrogen/oxygen fired, stoichiometric combustion with exhaust recirculation of steam under the rated temperature conditions of 1573K. An overall equivalence ratio was set at 1 with other conditions equivalent to the rated conditions in Table 1.

Hydrogen/oxygen reaction began as rapidly as in the cases of gasified fuel/O₂ or CH₄/air fired combustion, shown in Fig.10 or Fig.11, respectively. After that, hydrogen oxidation reaction progressed faster than in the case of gasified fuel/O₂ fired combustion.

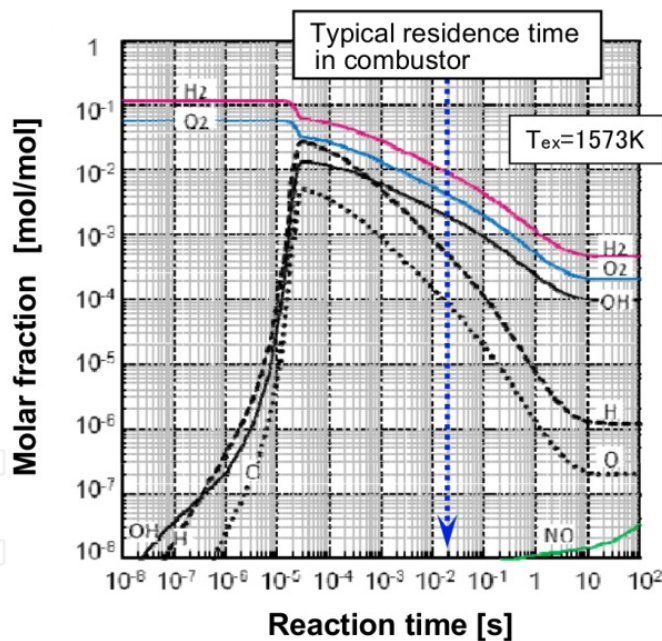


Figure 13. Chemical species behavior over time in H₂/O₂ combustion with steam recirculation

Figure 14 shows exhaust characteristics and combustion efficiencies under the conditions of a 1573K combustor exhaust temperature compared with the cases of homogeneous premixed combustions of H₂/O₂ and CH₄/O₂ mixture with exhaust recirculation. Here, we set the composition of each recirculating exhaust to that of corresponding gas formed under equilibrium conditions.

As an example of oxygen-fired gas turbine using stoichiometric combustion with exhaust recirculation, Fig.14 also shows comparative calculations with test data of 1973K-class H₂/O₂ stoichiometric combustion with steam recirculation, conducted in the Japanese WE-NET project. Tests confirmed that the analytical results were almost in accordance with experimental results [33] concerning concentrations of residual O₂ constituent and unburned H₂ constituent in exhaust, and that the numerical analysis used in this study could estimate emission characteristics under conditions of achieved high combustion efficiency.

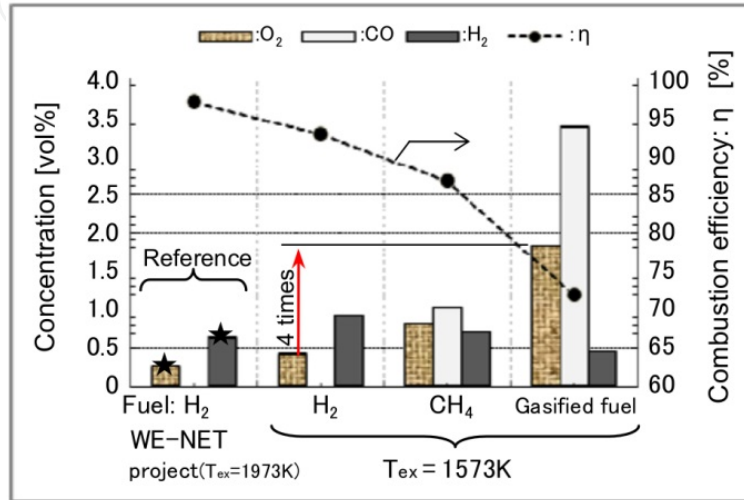


Figure 14. stoichiometric combustion characteristics of each fuel; overall equivalence ratio is 1, markers (★) are test data under conditions where combustion pressure is set at 2.5MPa and recirculated steam temperature is 623K [33].

In the case of H₂/O₂ fired combustion such as in a hydrogen fired closed-cycle gas turbine, emissions of combustible constituent H₂ and residual O₂ in exhaust decreased 1vol% or below in a reaction time of 20ms, or combustion efficiency was estimated to reach up to around 93% at a temperature of 1573K. In the case of a CH₄/O₂ fired, closed cycle gas turbine, combustible constituent CO and residual O₂ concentration of combustor exhaust also decreased 1vol% or below, and combustion efficiency reached 87%, while combustible contents and residual O₂ emissions displayed a tendency to increase compared to the H₂/O₂ fired combustion.

Combustible contents and residual O₂ emissions, on the other hand, increased by several times in the case of gasified fuels compared with both cases of H₂ fired and CH₄ fired combustion. Combustion efficiency fell to a low level of 72%. In CO-rich fuel/O₂-fired combustion with exhaust recirculation, CO oxidation was strongly restrained by recirculating exhaust consisting mostly of CO₂ compared to other fuel constituents, and combustion efficiency was decreased. Therefore, to achieve highly efficient oxy-fuel IGCC, it is necessary to develop combustion control technologies of gasified fuel/O₂ combustion with higher combustibility compared with the H₂/O₂ combustion technology in the WE-NET project or pre-combustion technologies.

4.3. Effects of fuel CO/H₂ molar ratio on emission characteristics

Each quantity of CO and H₂ constituent in the gasified fuels differs chiefly according to the gasification methods, raw materials of feedstock, and water-gas-shift reaction as an optional extra for pre-combustion carbon capture system. Figure 15 shows influences of CO/H₂ molar ratio in the gasified fuel on the combustion emission characteristics with exhaust recirculation under the rated temperature condition of 1573K. In the case of varying the fuel CO/H₂ molar ratio under the conditions where the total amount of CO and H₂ constituent was set constant, dilution ratio (dilution gas/fuel molar ratio) was adjusted to maintain the combustion temperature at 1573K. Just like the case of Fig.14, overall equivalence ratio was set at 1, with other conditions equivalent to the rated conditions in Table 1. In the case of changing the fuel CO/H₂ molar ratio from 2.8 of base condition to 0.36, the amounts of CO and H₂ constituent replaced each other under the condition where the total amount of CO and H₂ was set constant of 90vol%.

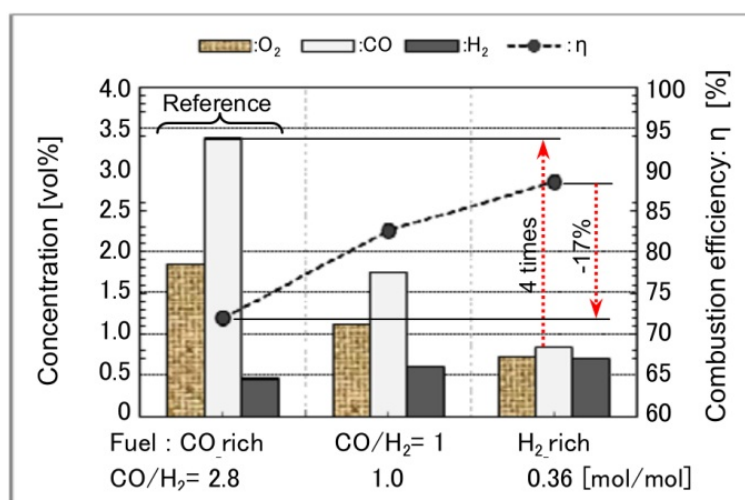


Figure 15. Effects of CO/H₂ molar ratio in fuel on stoichiometric combustion characteristics; overall equivalence ratio is 1. Notes: In the case of changing the fuel CO/H₂ molar ratio from 2.8 of base condition to 0.36, the amounts of CO and H₂ constituent replace each other under the condition where the total amount of CO and H₂ is set constant of 90vol%.

In the case of higher CO/H₂ molar ratio in the fuel, higher concentration of CO and lower concentration of H₂ in fuels increased CO emissions in combustion exhaust significantly, but have insignificant effects on reduction of H₂ emissions. As a result, in the case of CO rich gasified fuels, CO emissions increased four times those in the case of H₂ rich gasified fuel in the pre-combustion IGCC system, or combustion efficiency decrease by about 17%. This is explained both because H₂ is decomposed and produces OH, H and O radicals in the chain initiation as shown in Fig.10, and exhaust recirculation strongly inhibits oxidation of CO that is oxidized directly to CO₂ by the following reactions:



Furthermore, H₂ is oxidized more rapidly than CO, or CO constituent controls overall oxidation reaction rate of fuel in the stoichiometric combustion with exhaust recirculation. Consequently, when the CO/H₂ molar ratio increased, CO oxidation rate and O₂ consumption rate decreased.

4.4. Effects of equivalence ratio on emission characteristics

Figure 16 shows the effects of an equivalence ratio on combustion emission characteristics under the rated temperature 1573K. When varying the equivalence ratio, the dilution ratio (dilution gas/fuel molar ratio) was adjusted to maintain the combustion temperature at 1573K. The horizontal axis indicated an apparent equivalence ratio, ϕ^* calculated from fuel and an oxidizer without O₂ concentration in the dilution of recirculated exhaust. Emission features and combustibility of the combustor were characterized by combustion conditions near the burner. That is, Fig.16 indicated the influence of a so-called "local equivalence ratio" near the burner on combustion emission characteristics by using the apparent equivalence ratio ϕ^* .

In the case of decreasing ϕ^* from 0.98 to 0.95, combustion efficiency increased by only 5 percent, while overall equivalence ratio decreased from 0.89 to a low level of 0.75. That is, lowering the equivalence ratio could not result in any remarkable combustion promotion in CO-rich fuel/O₂ fired combustion with exhaust recirculation, while O₂ concentration in the exhaust significantly increased and the usage of exhaust to feed coal into the gasifier was restrained. It is necessary to decrease O₂ concentration in the carrier gas to feed coal by oxidation reactions using fuels such as hydrocarbons, or auxiliary power increased. Therefore, we have to decide the equivalence ratio in the combustor in consideration of the influence of residual O₂ on thermal efficiency of the whole system and performance of its equipments.

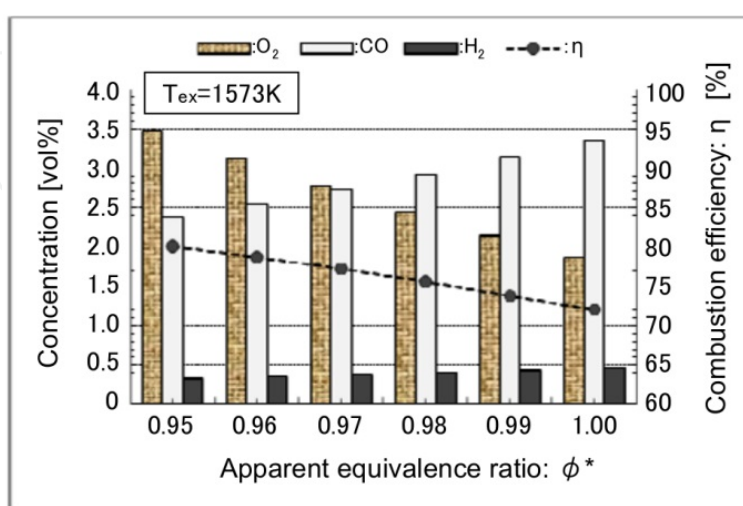


Figure 16. Effects of apparent equivalence ratio(ϕ^*) on combustion emission characteristics

4.5. Influences of oxygen concentration in oxidizer on emission characteristics

O_2 concentration in oxidizer derived from an air separation unit differs according to the air separation and purification system. Figure 17 shows influences of oxygen concentration in oxidizer on the combustion emission characteristics under the rated temperature conditions. In the case of varying the oxygen concentration in oxidizer, dilution ratio (dilution gas/fuel molar ratio) was adjusted to maintain the combustion temperature at 1573K and overall equivalence ratio at 1.0. The remainder of the oxidizer without O_2 was set to N_2 .

Emissions of residual O_2 and combustible constituents of CO and H_2 in exhaust tended to increase with the increase in oxygen concentration in oxidizer, or combustion efficiencies decreased. In the case of increasing O_2 concentration from 80vol% to 100vol%, combustion efficiency decreased by 13%, while residual concentrations of argon and nitrogen originated in air decreased. It was said that the non-condensable gases such as remaining O_2 , argon and nitrogen resulted in increased condensation duty for the recovery of the CO_2 [21], or influence of residual constituents on the whole system and its equipments must be examined separately.

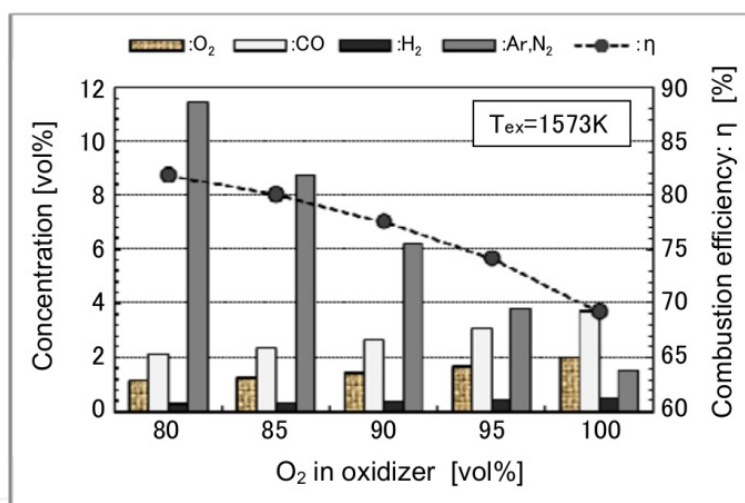


Figure 17. Effects of oxygen concentration in oxidizer derived from air separation unit on combustion emission characteristics; overall equivalence ratio is 1.

4.6. Reaction characteristics of gas turbine exhaust

Figure 18 shows a typical stream history of exhaust temperature and pressure from a gas turbine inlet to a compressor inlet of recirculating exhaust. Power was recovered from exhaust emanating from the combustor in the expansion turbine, and combustor exhaust temperature of 1573K with a pressure of 2.2MPa decreased to around 950K and 0.1MPa respectively at the turbine exit. Then, heat from expansion turbine exhaust was recovered through heat recovery steam generator (HRSG) in a flue, and exhaust temperature decreased to around 373K at the compressor inlet. In these analyses, we employed the PFR

model for the turbine exhaust to the compressor inlet, and assuming that species in exhaust is evenly mixed and that there is no distribution of temperature and pressure in the mixtures. There is also no supply of added oxidizer and recirculating exhaust in the reaction processes.

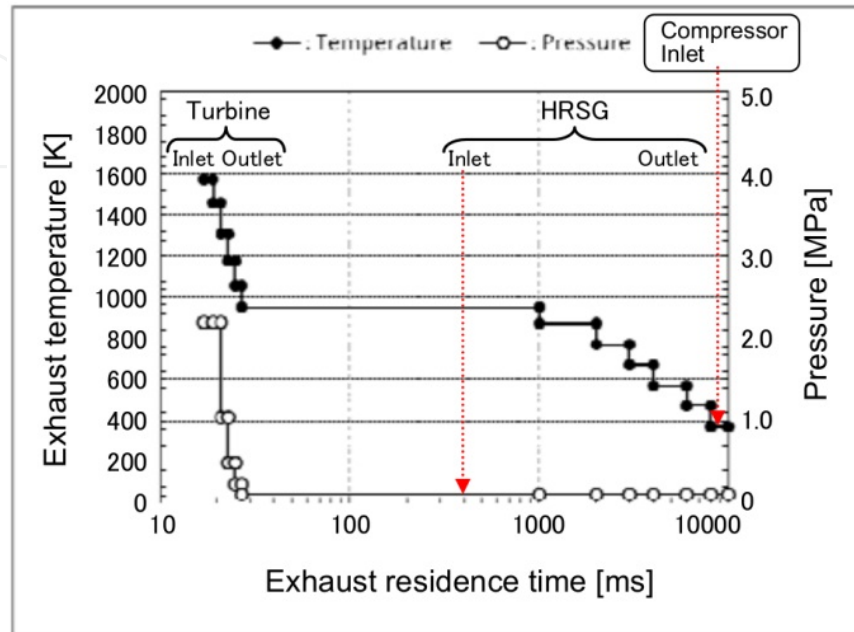


Figure 18. Typical stream history of exhaust temperature and pressure from gas turbine inlet to compressor inlet of recirculating exhaust

Figure 19 shows the reaction characteristics of combustion gas in the combustor and exhaust gas from combustor outlet to compressor inlet of recycled exhaust using a combination PSR and PFR model. CO and H₂ at high concentration in exhaust could be slowed to oxidize under the temperature conditions of an expansion turbine and HRSG. Combustible constituents of CO and H₂, and residual O₂ therefore decreased in concentration along the exhaust flow direction. Oxidation reactions of CO and H₂ then nearly halted when the exhaust temperature decreased to 673K or less.

Figure 20 shows emission characteristics of exhaust gases and combustion efficiencies at typical conditions based on the above reaction characteristics.

In a reaction time of 400ms corresponding to the residence time between combustor exit and HRSG inlet, combustible constituent CO and H₂ decreased less than 0.01vol%, and residual O₂ decreased to around 0.9vol%, while CO and H₂ concentration in combustor exhaust hovered at around 3vol% and 0.4vol%, respectively, and residual O₂ was at 2.3vol% under 20ms of typical combustion gas residence time in the combustor. Each oxidation reaction of combustible constituents in the turbine and the flue resulted in an increase in combustion efficiency of η by about 12%, respectively, or a combustion efficiency was estimated to reach a high level of around 99.8%. If the reaction time was from 4 to 10 seconds when the exhaust

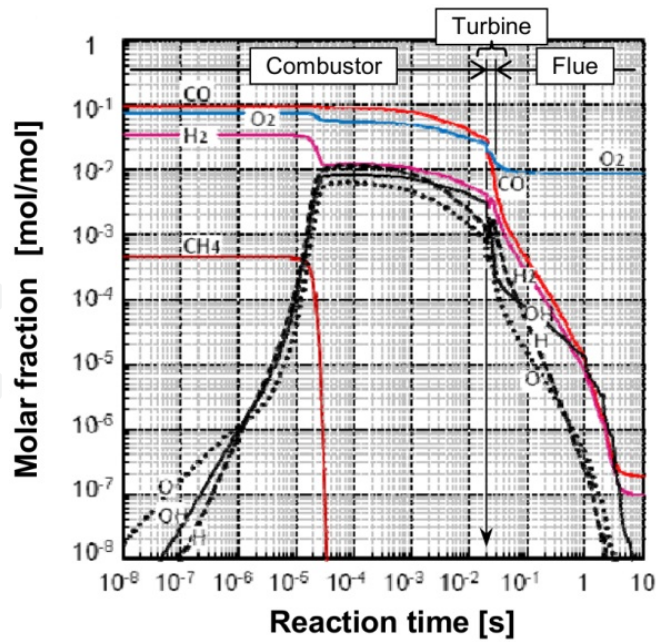


Figure 19. Chemical species behavior of combustion and exhaust gas over time in semiclosed cycle gas turbine, using PSR + PFR combined model. Combustor inlet conditions are the same as those in Fig.10 and flue includes HRSG.

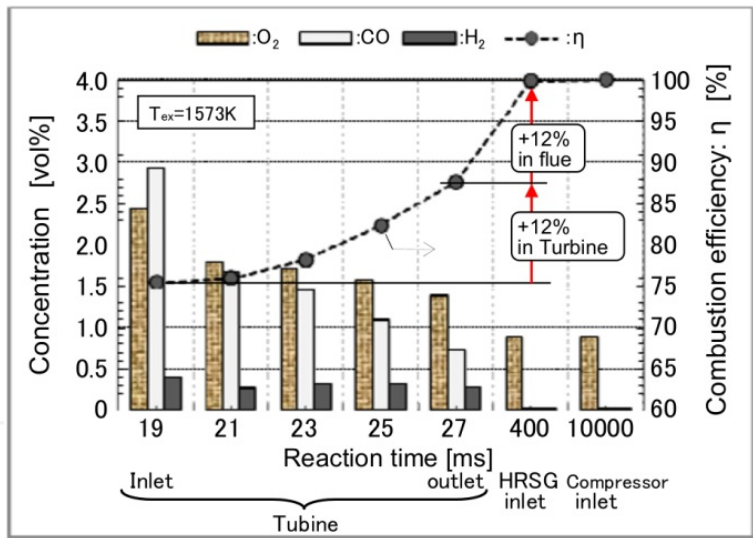


Figure 20. History of combustion emissions from gas turbine inlet to compressor inlet of recirculating exhaust

gas temperature decreased to around 673K in the HRSG, both combustible constituent CO and H₂ decreased to 10ppmv, or the combustion efficiency reached 100%.

From the abovementioned results, we were able to clearly slow combustible constituents in expansion turbine exhaust to oxidize under conditions of exhaust temperatures of over 673K, or recover burning energy from unburned fuel in HRSG. However, in this case, since reaction heat of combustible constituents in HRSG corresponds to a fuel for reheat type HRSG, some of the supplied fuel could not devote enough energy to a combined cycle ther-

mal efficiency. In order to achieve highly efficient oxy-fuel IGCC, it was therefore necessary to increase combustion efficiency as much as possible in the gas turbine combustor.

4.7. Influences of exhaust recirculation on thermal-NO_x emissions

As shown in Fig.20, it is found that combustible constituents reached almost equilibrium concentration at compressor inlet of recirculated exhaust, or that equilibrium gases were working fluids in the semiclosed cycle gas turbine. On the other hand, NO_x constituents increased by exhaust recirculation and were saturated by a balance between exhaust recirculation and CO₂ recovery process. Figure 21 demonstrates the influence of exhaust recirculation on thermal-NO emission characteristics through numerical analyses of a combination PSR and PFR model as in the case of Fig.20, with compositions of fuel and oxidizer shown in Table 1. In these analyses, Fig.21 indicates the direct effects of recirculating NO constituent on NO-saturating concentration under conditions where dilution gas composition without NO constituent is constant. That is, we repeated the calculation of one exhaust-recirculating loop shown in Fig.20, and investigated influence of exhaust recirculation on oxidation-reduction reaction of NO through full kinetic analyses. Combustion temperature was set at 1623K, and pressure at 3.0MPa; a little higher than indicated in Table 1. Dilution gas of recirculated exhaust at combustor inlet were set to equilibrium composition.

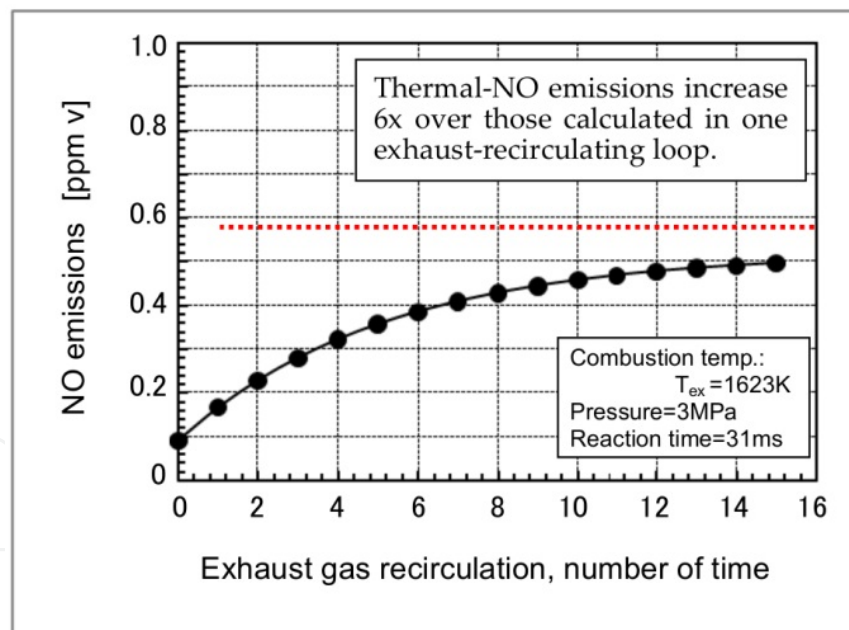


Figure 21. Influence of exhaust recirculation on thermal-NO emissions

Thermal-NO emissions increased in response to a number of times exhaust was recirculated and reached around 6 times higher than those calculated in one exhaust-recirculating loop, while NO production itself was not significantly large due to the small component amounts of N₂, as shown in Table 1. However, since thermal-NO production depends on reaction temperature, or thermal-NO emissions are strongly affected by both mixing processes and

non-uniformities of mixtures, we need further studies on thermal-NO emissions in the processes of combustion and combustor design.

5. Conclusions

Oxy-fuel IGCC employing an oxygen-fired, semiclosed cycle gas turbine with exhaust recirculation enables the realization of highly-efficient, zero-emissions power generation. Numerical analyses in this paper showed both combustion emission characteristics of the semiclosed cycle gas turbine combustor and oxidations of unburned fuel constituents in the turbine exhaust in a flue, compared with conventional air-fired gas turbines and advanced O₂-fired gas turbines. As a result, we were able in this study to clarify that unburned constituents in combustor exhaust were slow to oxidize under temperatures of over 673K in the flue and that all fuel energy could be used for power generation, while the oxidation reaction of CO-rich gasified fuel under stoichiometric conditions could be restrained with CO₂ constituents in re-circulated exhaust at decreased combustion efficiency. In this case, however, all the supplied fuel could not devote enough energy to boosting combined cycle thermal efficiency, leading therefore to a decrease in thermal efficiency overall. As a next step, we propose the need to promote oxidation reaction by developing combustion control technology for the improvement of plant thermal efficiency.

Nomenclature

Dilution ratio: dilution gas of exhaust recirculation over fuel supply ratio, [mol/mol]

HRSG: heat recovery steam generator

T_{ex}: average temperature of combustor exit gas, [K]

η: combustion efficiency, [%]

$$\text{combustion efficiency} = \left(1 - \frac{\text{combustor exhaust gas}[\text{mass flow} \times \text{lower heating value}]}{\text{gasified fuel supplied to combustor}[\text{mass flow} \times \text{lower heating value}] + \text{recirculated exhaust}[\text{mass flow} \times \text{lower heating value}]} \right) \times 100 \quad (4)$$

φ*: apparent equivalence ratio calculated from fuel and oxidizer without O₂ concentration in recirculating dilution gas, [-]

Acknowledgements

The author wishes to express their appreciation to the many people who have contributed to this investigation.

Author details

Takeharu Hasegawa

Address all correspondence to: takeharu@criepi.denken.or.jp

Central Research Institute of Electric Power Industry, Nagasaka, Yokosuka-Shi Kanagawa-Ken, Japan

References

- [1] BP Statistical Review, "Historical Statistical Data from 1965-2010" and "BP Statistical Review of World Energy 2011", <http://www.bp.com/statisticalreview/> (accessed on 13 March 2011).
- [2] for example, The Energy Data and Modelling Center, The Energy Conservation Center, Japan, 2010, "2010 EDMC Handbook of Energy & Economic Statistics in Japan", ISBN:978-4-87973-365-8.
- [3] Shirai, H., et al., 2007, "Proposal of high efficient system with CO₂ capture and the task on integrated coal gasification combined cycle power generation," Central Research Institute of Electric Power Industry (CRIEPI) Report No.M07003. (in Japanese)
- [4] Nakao, Y., et al., 2009, "Development of CO₂ capture IGCC system -Investigation of aiming at higher efficiency in CO₂ capture IGCC system-," CRIEPI report No.M08006. (in Japanese)
- [5] Hasegawa, T., et al., 2011, "Study on gas turbine combustion for highly-efficient IGCC power generation with CO₂ capture -2nd report: emission analysis of gasified-fueled gas turbines with circulating exhaust & stoichiometric combustion-," CRIEPI report No.M10005, ISBN:978-4-7983-0462-5. (in Japanese)
- [6] Hasegawa, T., 2012, "Combustion Performance in a Semi-Closed Cycle Gas Turbine for IGCC Fired with CO-Rich Syngas and Oxy-Recirculated Exhaust Streams," Trans. ASME, J. Eng. Gas Turbines Power, Vol.134?, Issue *, pp.***-***, ISSN:0742-4795. (in press)
- [7] Kobayashi, M., et al., 2009, "Optimization of dry desulfurization process for IGCC power generation capable of carbon dioxide capture -determination of carbon deposition boundary and examination of countermeasure-," CRIEPI report No.M09015. (in Japanese)
- [8] Umemoto, S., et al., 2010, "Modeling of coal char gasification in coexistence of CO₂ and H₂O," Proceedings of The 27th Annual International Pittsburgh Coal Confer-

- ence, The University of Pittsburgh, Hilton Istanbul, Istanbul, TURKEY (13 October 2010).
- [9] Kidoguchi, K., et al., 2011, "Development of oxy-fuel IGCC system with CO₂ recirculation for CO₂ capture -experimental examination on effect of gasification reaction promotion by CO₂ enriched using bench scale gasifier facility-, " Proceedings of the ASME Power Conference 2011 and the International Conference on Power Engineering 2011 (14 July 2011).
 - [10] Engineering Advancement Association of Japan, WE-NET Home Page/WE-NET report, http://www.ena.or.jp/WE-NET/report/report_j.html (accessed on 12 March 2011).
 - [11] Ciferno, J.P., et al., 2010, "DOE/NETL carbon dioxide capture and storage RD&D roadmap (December 2010)," available online: http://www.netl.doe.gov/technologies/carbon_seq/refshelf/CCSRoadmap.pdf (accessed on 13 September 2011).
 - [12] Ciferno, J.P., et al., 2011, "DOE/NETL Advanced CO₂ Capture R&D Program: Technology Update, May 2011 Edition," available online: <http://www.netl.doe.gov/technologies/coalpower/ewr/pubs/CO2CaptureTechUpdate051711.pdf> (accessed on 1 November 2011).
 - [13] Bancalari, Ed., Chan, P., and Diakunchak, I.S., 2007, "Advanced hydrogen gas turbine development program," Proceedings of the ASME Turbo Expo 2007: Power for Land, Sea and Air GT2007, ASME paper GT2007-27869, Montreal, Canada, May 14-17, 2007.
 - [14] Todd, D.M. and Battista, R.A., 2000, "Demonstrated applicability of hydrogen fuel for gas turbines," Proceedings of the IChemE "Gasification 4 the Future" Conference, Noordwijk, the Netherlands, April 11-13, 2000.
 - [15] Kajitani, S., Suzuki, N., Ashizawa, M., and Hara, S., 2006, "CO₂ gasification rate analysis of coal char in entrained flow coal gasifier," Fuel 85, pp.163-169.
 - [16] Nunokawa, M., Kobayashi, M., Shirai, H., 2008, "Halide compound removal from hot coal-derived gas with reusable sodium-based sorbent," Powder Technology, 180(1-2), pp.216-221.
 - [17] Akiho, H., Kobayashi, M., Nunokawa, M., Tochiara, Y., Yamaguchi, T., Ito, S., 2008, "Development of Dry Gas Cleaning System for Multiple Impurities -Proposal of low-cost mercury removal process using the reusable absorbent -," Central Research Institute of Electric Power Industry, Report No.M07017. (in Japanese)
 - [18] Ozawa, Y. and Tochiara, Y., 2010, "Study of Ammonia Decomposition in Coal Derived Gas - Decomposition Characteristics over Supported Ni Catalyst -, " Central Research Institute of Electric Power Industry, Report No.M09002. (in Japanese)
 - [19] Nunokawa, M., Kobayashi, M., Nakao, Y., Akiho, H., Ito, S., 2010, "Development of gas cleaning system for highly-efficient IGCC -Proposal for scale-up scheme of optimum

gas cleaning system based on generating efficiency analysis-," Central Research Institute of Electric Power Industry, Report No.M09016. (in Japanese)

- [20] for example; Hasegawa,T., 2006, "Gas turbine combustor development for gasified fuels and environmental high-efficiency utilization of unused resources," Journal of the Japan Petroleum Institute, Vol.49, No.6, pp.281-293.
- [21] Li,H., Yan,J., and Anheden,M., 2009, "Impurity impacts on the purification process on Oxy-fuel combustion based on CO₂ capture and storage system," Appl. Energy 2009; 86, pp.202-213.
- [22] Miller,J.A. and Bowman,C.T., 1989, "Mechanism and modeling of nitrogen chemistry in combustion," Prog. Energy Combust. Sci., vol.15, pp.287-338.
- [23] Hasegawa,T., et al., 1998, "Study of ammonia removal from coalgasified Fuel," Combust. Flame 114, pp.246-258.
- [24] Lyon,R.K., 1979, "Thermal DeNO_x: how it works," Hydrocarbon Processing 1979 (ISSN 0018-8190), Gulf Publishing Co., Houston, Texas, (October 1979), vol.59, No.10, 109-112.
- [25] Hasegawa,T., Sato,M., Sakuno,S., and Ueda,H., 2001, "Numerical Analysis on Application of Selective Non Catalytic Reduction to Wakamatsu PFBC Demonstration Plant", Paper number : JPGC2001/FACT-19052, Presented at the 2001 International Joint Power Generation Conference, New Orleans, Louisiana, U.S.A., 2001-6-6.
- [26] Nakata T., Sato M., and Hasegawa T., 1998, "Reaction Kinetics of Fuel NO_x Formation for Gas Turbine conditions", Trans. ASME, J. Eng. Gas Turbines Power, Vol.120, No.3, pp.474-480.
- [27] Hasegawa,T., et al., 1997, "Fundamental Study On Combustion Characteristics Of Gas Turbine Using Oxygen-Hydrogen -Numerical Analysis Of Formation/Destruction Characteristics Of Hydrogen, Oxygen And Radicals-," CRIEPI report No.W96007. (in Japanese)
- [28] C.Y. Liu, G. Chen, N. Sipöcz, M. Assadi, X.S. Bai, 2012, "Characteristics of oxy-fuel combustion in gas turbines," Applied Energy, Volume 89, Issue 1, January 2012, pp. 387-394.
- [29] Chase, Jr.M.W.; Davies, C.A.; Downey, Jr.J.R.; Frurip, D.J.; McDonald, R.A.; Syverud, A.N., 1985, "JANAF Thermodynamical Tables, 3rd Edition.," J. Phys. Chem. Reference Data, Vol.14.
- [30] Kee,R.J., Rupley,F.M., and Miller,J.A., 1990, "The CHEMKIN Thermodynamic Data Base," Sandia Report, SAND 878215B.
- [31] Hindmarsh,A.C., 1974, "GEAR: Ordinary differential equation system solver," Lawrence Livermore Laboratory, Univ. California, Report No. UCID30001, Rev.3.

- [32] Pratt, D.T.; Bowman, B.R.; Crowe, C.T. Prediction of Nitric Oxide Formation in Turbojet Engines by PSR Analysis. AIAA paper 1971, No.71-713.
- [33] Engineering Advancement Association of Japan, WE-NET Home Page/WE-NET report, <http://www.ena.or.jp/WE-NET/report/1998/japanese/gif/823.htm#823> (accessed on 12 March 2012).

IntechOpen

IntechOpen